ACS Medicinal Chemistry Letters

pubs.acs.org/acsmedchemlett Letter

Design, Synthesis, and Biological Evaluation of Selective CDK4/9 Inhibitors

Siqi Li,[§] Xiaotang Yang,[§] Weiyi Yin, Wencui Zhang, Zhuorong Li,* Jinping Hu,* and Yanping Li*

Cite This: https://doi.org/10.1021/acsmedchemlett.6c00004 Read Online

ACCESS | Metrics & More | Article Recommendations | Supporting Information

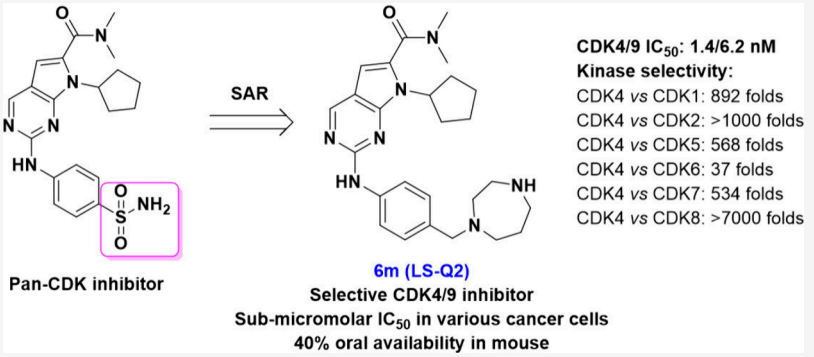

ABSTRACT: Simultaneous inhibition of cell cycle CDKs and transcriptional CDKs may provide a novel strategy for cancer therapy. Starting from a pan-CDK inhibitor, a series of novel 2-((4-substitutedphenyl)amino)-pyrrolo[2,3-*d*]pyrimidine derivatives were synthesized and evaluated for their inhibition effects on cellular proliferation and CDK enzymatic activity. Several new derivatives exhibited significantly improved profiles in terms of *in vitro* antitumor potency, metabolic stability, and kinase selectivity. Further biological and *in vivo* pharmacokinetic evaluation confirmed that derivative **6m** (LS-Q2) is a novel, orally bioavailable, and highly selective CDK4/9 inhibitor with potent antiproliferative activity against various tumor cells. Moreover, LS-Q2 exhibited significant synergistic antitumor effects when combined with the BET and Bcl-2 inhibitors. The discovery of LS-Q2 provides promising next-generation CDK inhibitor leads for the treatment of malignant solid tumors beyond breast cancer and highlights the potential of orally available and selective CDK4/9 inhibitors in cancer treatment.

KEYWORDS: *pyrrolo[2,3-d]pyrimidine derivatives, CDK4/9 inhibitors, synthesis, antiproliferation, structure−activity relationship*

The global cancer burden remains heavy, despite breakthrough advances in antitumor therapy in recent decades. Treatment options for patients with advanced or unresectable tumors continue to be limited, especially for cancers with hidden onset and advanced diagnosis. For example, hepatocellular carcinoma (HCC) accounts for approximately 75−85% of primary liver cancers in China.[1,2] Both multitargeted tyrosine kinase inhibitors (TKIs) such as sorafenib and lenvatinib and immune checkpoint inhibitors, including anti-PD-1 antibodies, have significantly improved the median overall survival of patients with unresectable HCC.[3−8] However, these regimens are still plagued by challenges such as low objective response rates, adverse effects, and drug resistance.[9,10] The situation is even more critical in pancreatic cancer, where FOLFOX-based chemotherapy is widely adopted in the real world to control tumor progression, yet the overall five-year survival rate remains below 10%.[11] Therefore, continued efforts are urgently required for developing new anticancer drugs until curable therapies become available.

Cyclin-dependent kinases (CDKs) are a family of serine/threonine protein kinases whose members are primarily divided into two groups according to their cellular functions: cell-cycle CDKs, such as CDK1, 2, 4, 6, 7, and transcriptional CDKs, including CDK7, 8, and 9.[12] Functional dysregulation of CDKs is a common feature of human tumors, and has been implicated in cancer initiation and progression.[13−16] Following the approval of selective inhibitors of cell cycle CDK4 and CDK6 by the US Food and Drug Administration (FDA) or China's National Medical Products Administration (NMPA), the clinical value of selective CDK inhibitors in cancer therapy has become evident. Combination regimens involving these CDK4/6 inhibitors and endocrine therapy have dramatically

Received: January 2, 2026
Revised: March 22, 2026
Accepted: March 23, 2026

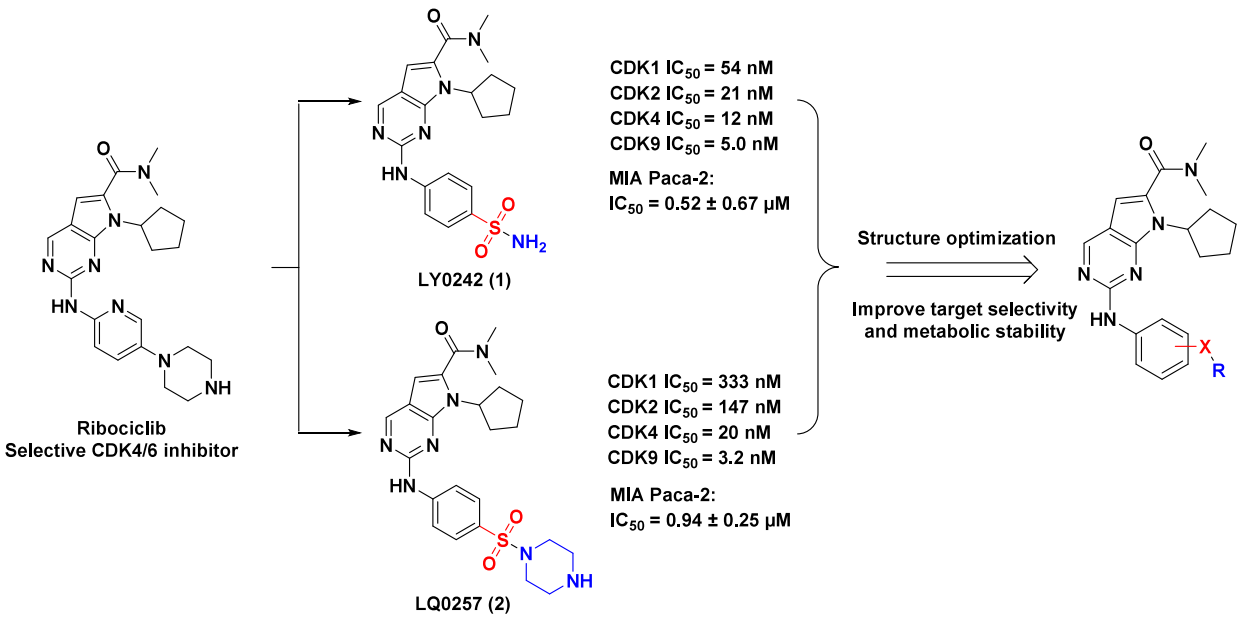

Figure 1. Structural optimization of 2-substituted pyrrolo[2,3-*d*]pyrimidine derivatives.

Scheme 1. Synthetic Routes of 2-((Substitutedphenyl))amino-7-cyclopentyl-N,N-dimethyl-7H-pyrrolo[2,3-*d*]pyrimidine-6-carboxamide Derivatives[a]

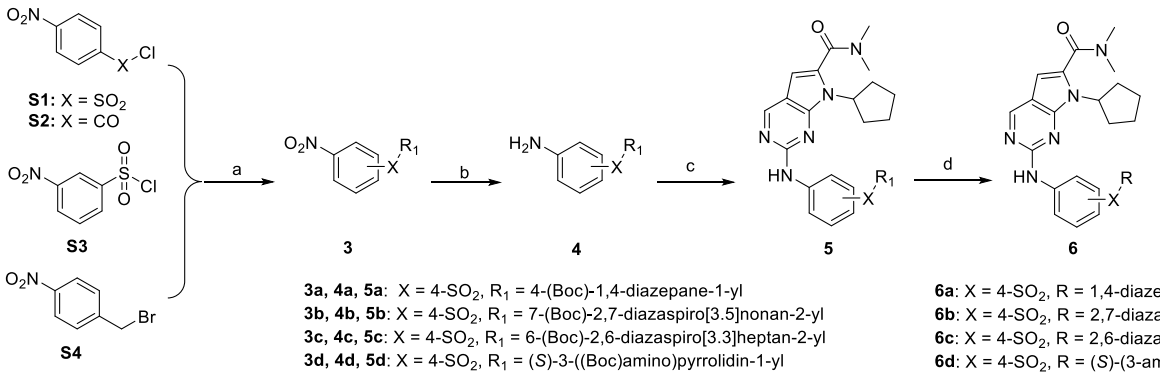

3a, 4a, 5a: X = 4-SO_2, R_1 = 4-(Boc)-1,4-diazepane-1-yl
3b, 4b, 5b: X = 4-SO_2, R_1 = 7-(Boc)-2,7-diazaspiro[3.5]nonan-2-yl
3c, 4c, 5c: X = 4-SO_2, R_1 = 6-(Boc)-2,6-diazaspiro[3.3]heptan-2-yl
3d, 4d, 5d: X = 4-SO_2, R_1 = (*S*)-3-((Boc)amino)pyrrolidin-1-yl
3e, 4e, 5e: X = 4-SO_2, R_1 = *N*-(1-(Boc)pyrrolidin-3-yl)-*N*-methyl
3f, 4f, 5f: X = 4-SO_2, R_1 = 3-(Boc)-3,8-diazabicyclo[3.2.1]octan-8-yl
3g, 4g, 5g: X = 4-SO_2, R_1 = 5-(Boc)-2,5-diazabicyclo[2.2.2]octan-2-yl
3h, 4h, 5h: X = 3-SO_2, R_1 = 4-(Boc)-1,4-diazepane-1-yl
3i, 4i, 5i: X = 4-SO_2, R_1 = 4-(Boc)-2-methylpiperazin-1-yl
3j, 4j, 5j: X = 4-CO, R_1 = 4-(Boc)-2-methylpiperazin-1-yl
3k, 4k, 5k: X = 4-CH_2, R_1 = 4-(Boc)-2-methylpiperazin-1-yl
3l, 4l, 5l: X = 4-CO, R_1 = 4-(Boc)-1,4-diazepane-1-yl
3m, 4m, 5m: X = 4-CH_2, R_1 = 4-(Boc)-1,4-diazepane-1-yl

6a: X = 4-SO_2, R = 1,4-diazepane-1-yl
6b: X = 4-SO_2, R = 2,7-diazaspiro[3.5]nonan-2-yl
6c: X = 4-SO_2, R = 2,6-diazaspiro[3.3]heptan-2-yl
6d: X = 4-SO_2, R = (*S*)-(3-aminopyrrolidin-1-yl)
6e: X = 4-SO_2, R = *N*-methyl-*N*-(pyrrolidin-3-yl
6f: X = 4-SO_2, R = 3,8-diazabicyclo[3.2.1]octan-8-yl
6g: X = 4-SO_2, R = 2,5-diazabicyclo[2.2.2]octan-2-yl
6h: X = 3-SO_2, R = 1,4-diazepane-1-yl
6i: X = 4-SO_2, R = 2-methylpiperazin-1-yl
6j: X = 4-CO, R = 2-methylpiperazin-1-yl
6k: X = 4-CH_2, R = 2-methylpiperazin-1-yl
6l: X = 4-CO, R = 1,4-diazepane-1-yl
6m: X = 4-CH_2, R = 1,4-diazepane-1-yl

[a]Reagents and conditions: (a) N^1-Boc-diazacycloalkane, K_2CO_3, DCM, 80%; (b_1) Pd/C, H_2 (35 psi), MeOH, 90%; (b_2) Fe, NH_4Cl, EtOH/H_2O, 65%; (c) 2-chloro-7-cyclopentyl-N,N-dimethyl-7H-pyrrolo[2,3-*d*]pyrimidine-6-carboxamide, Xantphos, $Pd_2(dba)_3$, Cs_2CO_3, toluene, 110 °C, microwave irradiation; (d) concentrated hydrochloride aqueous solution, MeOH, 70 °C.

improved clinical outcomes for patients with hormone receptor-positive (HR+), HER2-negative (HER2-) advanced breast cancer. However, the application of these CDK4/6 inhibitors alone in tumors beyond breast cancer remains challenging, as the current success of CDK4/6 inhibitors relies on overexpression of cyclin D in HR+ breast cancer.[17] A number of clinical trials are investigating the potential of combining CDK4/6 inhibitor with other drugs to treat diverse malignancies.[18−20] CDK9 is a predominant member of the transcriptional CDKs subfamily.[21] The CDK9-cyclin T complex is the regulatory subunit of positive transcription elongation factor b (P-TEFb), which phosphorylates the C-terminal domain (CTD) of RNA polymerase II and promotes the elongation of mRNA transcripts.[22] CDK9 has been considered as a potential therapeutic target in various diseases, including cancers.[23−26] Our previous study suggests that simultaneous inhibition of CDK4 and CDK9 is important for suppressing pancreatic cancer cell growth.[27] This is consistent with the initial discovery reported by Cai et al, which demonstrated that combined depletion of cell cycle and transcriptional CDK activities induced substantial apoptosis in cancer cells.[28] Here, we report a novel, highly selective CDK4/9 inhibitor that exhibits potent antiproliferative activity and oral bioavailability, representing a promising candidate for the treatment of various solid tumors.

https://doi.org/10.1021/acsmedchemlett.6c00004
ACS Med. Chem. Lett. XXXX, XXX, XXX−XXX

2-((4-Sulfamoylphenyl)amino)-pyrrolo[2,3-*d*]pyrimidine derivative **1** (Figure 1) was previously identified as a CDK9 inhibitor, exhibiting significantly enhanced antiproliferative activity in pancreatic cancer cells compared to CDK4/6 inhibitor ribociclib.[27] However, the miscellaneous inhibition effect on multiple CDKs and low systemic exposure after oral administration to animals were observed. Further expanding the terminal sulfonamide of compound **1** to a bulkier sulfonylpiperazine (**2**) increased kinase selectivity toward CDK4 and CDK9 without affecting the antiproliferative activity. However, methylation of the piperazine in compound **2**, or the displacement of piperazine with piperidine or morpholine, reduced both CDK inhibition and antiproliferative activity. These results suggest that the terminal sulfonamide moiety could be a handle for improving kinase selectivity and that a free NH group at this position is important for maintaining pharmacological activity (Figure 1). Thus, a series of saturated diazacycles were first introduced to replace the terminal group at the 2-position of compound **2**, yielding diverse piperazine-superseded derivatives to investigate the steric effects of substituents. To further explore the steric and electronic effects on oral absorption, the terminal sulfamoyl group was systematically modified by introducing a 2-methylpiperazine, varying the sulfonamide position, or replacing the sulfonyl group with formyl or methylene.

All new derivatives were synthesized using previously described methods with slight modifications.[27] As shown in Scheme 1, starting from 4-nitrobenzenesulfonyl chloride, various N^1-Boc-diazacycloalkanes were converted to the corresponding sulfonamide intermediates **3a**−**3g** via an acylation reaction. Subsequent hydrogenation reduction afforded the 4-sulfonamide-aniline intermediates **4a**−**4g** in an overall two-step yield of 70%. Finally, Pd-catalyzed coupling of **4a**−**4g** with the commercially purchased 2-chloro-7-cyclopentyl-N,N-dimethyl-7H-pyrrolo[2,3-*d*]pyrimidine-6-carboxamide, followed by removal of the Boc protecting group, yielded the target piperazine-superseded derivatives **6a**−**6g**, respectively. Starting from 3-nitrobenzenesulfonyl chloride or 4-benzoyl chloride, the 3-sulfonamide derivative **6h** and the 4-benzamide derivative **6j** and **6l** were prepared using the same method as for **6a**−**6g**. For the methylene-linked analogs (X = CH_2), 4-nitrobenzyl bromide was used for the N-alkylation of N-Boc-diazacycloalkanes to afford intermediates **3k** and **3m**. Subsequent reduction of the nitro group in the presence of ammonium chloride and iron powder gave intermediates **4k** and **4m** in the yield of 60%. Finally, diazacycloalkyl benzylamine derivatives **6k** and **6m** were prepared by Pd-catalyzed coupling followed by the deprotection of the Boc group.

All synthetic piperazine-superseded pyrrolo[2, 3-d]-pyrimidine derivatives were screened for their inhibitory effect on both cell viability of liver cancer HepG2 cells and CDK9/cyclin T kinase activity. As shown in Table 1, the reference compound **2** exhibited significant antiproliferative activity on cancer cell growth at submicromolar concentrations (IC_{50} = 0.46 μM). Replacing the piperazine group with a seven-membered 1,4-diazepane (**6a**, IC_{50} = 1.47 μM) resulted in approximately 3-fold lower potency compared to compound **2**. Two derivatives containing a 3-aminopyrrolidine moiety linked to the sulfonyl group via different nitrogen atoms (**6d** and **6e**) showed two-fold lower activity than **6a**. When piperazine was displaced by an extended spiral ring while the N atom connected with sulfonyl group was located within a four-membered ring, the antiproliferative activity of resulting compounds was more significantly reduced (**6b**, IC_{50} = 11.45 μM) or even lost (**6c**, IC_{50} > 50 μM). Introduction of a hydrophobic five- or six-membered fused ring to the piperazine also led to several-fold decreased potency. The compound bearing a five-membered fused ring (**6f**, IC_{50} = 1.56 μM) exhibited slightly stronger potency in HepG2 cells than its analogue bearing a six-membered fused ring (**6g**, IC_{50} = 3.75 μM). These results suggest that steric hindrance of the R group affects antiproliferative activity, with planar rings being more favorable than bulkier ones.

Table 1. Biological Screening of 2-((Sulfamoylphenyl)amino)-pyrrolo[2,3-*d*]pyrimidine Derivatives

Cpd.	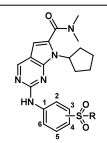		Anti-proliferation	CDK9 inhibition	LMS[b]	
	Position	R	IC_{50} (μM)	IC_{50} (nM)	Mouse	Human
2	C4-		0.46 ± 0.09	1.7	18%	35%
6a	C4-		1.47 ± 0.41	8.0	56%	74%
6b	C4-		11.45 ± 1.04	21.7	67%	91%
6c	C4-		> 50	ND[a]	ND	ND
6d	C4-		3.02 ± 0.12	9.2	29%	72%
6e	C4-		2.46 ± 0.37	10.5	60%	44%
6f	C4-		1.56 ± 0.38	11.4	3.9%	8.5%
6g	C4-		3.75 ± 0.46	13.2	38%	63%
6h	C3-		2.73 ± 0.55	15.0	1.8%	ND
Sorafinib			2.64 ± 0.31			

[a]ND means not determined. [b]The value represents the remaining percentage of test compound after 30 min incubation with LM.

The active piperazine-superseded pyrrolo[2,3-*d*]pyrimidine derivatives were evaluated for CDK9/cyclin T inhibitory activity in a Lance Ultra assay. These newly synthesized analogs displayed weaker CDK9 inhibitory activity (IC_{50} = 8.0 ∼ 21.7 nM) than that of compound **2** (IC_{50} = 1.7 nM), consistent with their antiproliferative activity. However, not all analogues exhibited a positive correlation between their antiproliferative activities and their CDK9 inhibitory activities (Table 1). Therefore, other CDK enzymatic inhibition might contribute to the antiproliferative potency.

These compounds were also investigated for liver microsome stability (LMS). As shown in Table 1, most of compound **2** was metabolized within 30 min in both mouse and human liver microsome solution, whereas compounds **6a**, **6b**, **6d**, **6e**, and **6g** exhibited higher metabolic stability (higher remaining percentage) than compound **2**. Notably, shifting the sulfonamide tail from the *para*-position to the *meta*-position of the benzene ring (**6h**) resulted in deterioration across all biological data, indicating that *para*-substitution of the benzene ring should be maintained. Moreover, a comprehensive analysis of antiproliferative activity, CDK9 inhibition, and LMS of above compounds suggests that homopiperazine can

https://doi.org/10.1021/acsmedchemlett.6c00004
ACS Med. Chem. Lett. XXXX, XXX, XXX−XXX

serve as an alternative to piperazine. Additionally, comparison of the LMS data for compounds **2**, **6f**, and **6g** suggests that introducing a substituent adjacent to the piperazine N1-position may improve the metabolic stability.

Encouraged by the above structure−activity relationship (SAR) study, we performed a second round of structural optimization. As expected, introducing an *ortho*-methyl group on the piperazine (**6i**) led to higher LMS compared to compound **2** (Table 2). Considering that ribociclib lacks the X group and possesses good oral availability, we further investigated the effect of the sulfonyl group on LMS by replacing it with carbonyl and methylene groups. When R is 2-methyl piperazine, the analogue with a carbonyl linker (**6j**) exhibited lower metabolic stability in mouse liver microsome solution than sulfonyl-linked compound **6i** and methylene-linked compound **6k**. However, the opposite is true when R is homopiperazine: the carbonyl compound **6l** showed higher stability than the methylene analog **6m**. This inverse relationship was also observed in the antiproliferation activity results: **6j** and **6m** demonstrated stronger anticancer potency (IC_{50} = 0.85 ∼ 0.88 μM) than **6k** (IC_{50} = 1.28 μM) and **6l** (IC_{50} = 2.28 μM), respectively, in HepG2 cells. Furthermore, replacement of the sulfonyl group with carbonyl or methylene resulted in significantly enhanced CDK4 inhibition, no matter if R is 2-methyl piperazine or homopiperazine. This suggests that a less steric X group is more favorable for binding to the CDK4 cavity. Moreover, less steric X groups also contributed to improved metabolic stability since both compounds **6l** and **6m** demonstrated equally favorable stability in the human liver microsome assay.

Table 2. In Vitro Biological Screening of 2-((4-Substitutedphenyl)amino)-pyrrolo[2,3-*d*]pyrimidine Derivatives

Cpd.	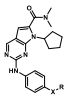		Anti-proliferation IC_{50} (μM)	IC_{50} (nM)		LMS*	
	X	R		CDK4	CDK9	Mouse	Human
2	-SO_2		0.57 ± 0.03	8.9	1.8	18.4%	35.0%
6i	-SO_2		1.25 ± 0.12	8.2	9.1	35.1%	ND
6j	-CO		0.88 ± 0.10	1.6	19.4	28.9%	ND
6k	-CH_2		1.28 ± 0.02	3.0	9.3	56.8%	ND
6l	-CO		2.28 ± 0.14	1.1	4.8	60.3%	70.8%
6m	-CH_2		0.85 ± 0.10	1.4	6.2	36.6%	73.3%

*The value represents the remaining percentage of test compound after 30 min incubation with LM.

During the preparing of this manuscript, Maddeboina et al. reported the discovery of LCI133, a potent multikinase (CDK4/6/9-AURKA/B) inhibitor with the same core structure as our compounds.[30] Therefore, we also determined the IC_{50} values of our candidate compounds against AURKA. Three compounds exhibited inhibitory activity against AURKA much weaker than that against CDK4/9, suggesting that new derivatives are selective inhibitors of CDK4 and CDK9. Among them, compound **6m** demonstrated the highest selectivity for CDK4/9.

We employed *in silico* molecular docking to compare the binding modes of CDK4/6 inhibitor ribociclib and compound **6m** in ATP-binding cavity of CDK9 and CDK6. As shown in Figure 2, ribociclib and compound **6m** presented similar poses within the ATP cavities of CDK9 and CDK6. The 2-aminopyrimidine moiety of these compounds formed typical hydrogen bonds with the hinge residues of CDK9 (CYS106) and CDK6 (HIS100, VAL101). In CDK9, the $\pi-\pi$-stacked interaction was shown between the pyrimidine ring and the gatekeeper residue PHE105 of CDK9 for both compounds. The carbonyl group substituted on the pyrrole ring and the terminal amino group of the homopiperazine of **6m** formed two additional H-bonds with an inner residue (ASP167) in the cavity and ILE25, a solvent-exposed residue in the G-loop region, respectively (Figure 2A). In all ribociclib-CDK9 complexes, no hydrogen bonds were observed in the terminal solvent region, while one configuration showed hydrogen bond formation between the carbonyl group and the deep residue LYS48. Therefore, the external H-bond in the solvent region

Table 3. Kinase Inhibition Screening of Three New Analogues

Cpd.	6k		6l		6m	
Kinase	IC_{50} (nM)	Fold vs CDK4	IC_{50} (nM)	Fold vs CDK4	IC_{50} (nM)	Fold vs CDK4
CDK4	3.0		1.1		1.4	
CDK9	9.3	**3**	4.8	**4**	6.2	**5**
CDK1	1597	**532**	205	**186**	1249	**892**
CDK2	1752	**584**	92	**83**	1491	**1065**
CDK5	865	**288**	54	**49**	795	**568**
CDK6	107	**35**	31	**28**	52	**37**
CDK7	2163	**721**	2579	**2344**	748	**534**
CDK8	>10000	**>3333**	>10000	**>9091**	>10000	**>7142**
AURKA	389	**130**	74	**52**	212	**212**

https://doi.org/10.1021/acsmedchemlett.6c00004
ACS Med. Chem. Lett. XXXX, XXX, XXX−XXX

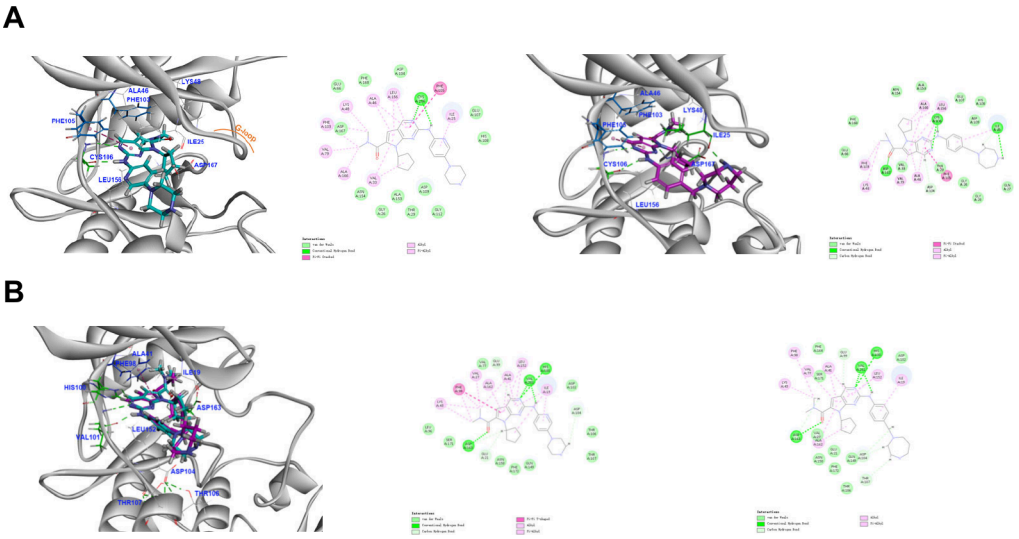

Figure 2. Binding mode of **6m** in the ATP-binding sites of the CDK kinase. The crystal structures of CDK9 (A, PDB ID: 4BCG) and CDK6 (B, PDB ID: 8I0M) were used for molecular docking of ribociclib (cyan sticks) and compound **6m** (purple sticks). Representative 3D and 2D interaction diagrams were produced by the Discovery Studio program.

contributed to the increased inhibitory activity of **6m** against CDK9 compared to ribociclib. As for CDK6, the only difference was that the pyrrole ring formed a $\pi-\pi$ interaction with the gatekeeper PHE98 in most of the ribociclib-CDK6 complex conformations, whereas **6m** did not exhibit this interaction at all (Figure 2B). Notably, the overall docking energy scores of the 10 conformations of the compound **6m**-CDK6 complex were all lower than those of the ribociclib-CDK6 complex. Jiang et al. synthesized and discovered selective CDK4/9 inhibitors by replacing the C2-substituent of ribociclib with 1,4-diaminocyclohexane, and deduced that the intramolecular hydrogen bonds formed within the unique DTT motif (ASP104, THR106, and THR107) in CDK6 impeded the interactions with their short-tail ligands, thereby increased the kinase selectivity versus CDK6.[31] Both Jiang's compounds and **6m** have the same core structure as ribociclib, and **6m** also exhibited increased CDK4 selectivity over CDK6 compared to ribociclib though it contains a longer tail. As shown in Figure 2B, the homopiperazine ring of compound **6m** formed weak CH−O bonds with ASP104 and THR107 of the DTT motif while ribociclib formed the CH−O with ASP104 and van der Waals interactions with THR106 and THR107, respectively. And a slightly longer distance of CH−O bond between heterocyclic CH group and ASP104 was observed for **6m** (2.66 Å) than ribociclib (2.57 Å). However, we are uncertain whether the increased CDK selectivity of **6m** over CDK6 originates from the effect of the DTT motif. We also simulated the binding modes of hit compound **1** and compound **6m** with the CDK2 protein in this work. Though both compounds are capable of binding to the ATP-binding site, their greater distance from the hinge region of CDK2 prevents the formation of polar interactions with the hinge residues (Figure S1). A unique hydrogen bond between the short sulfonamide moiety of compound **1** and residue GLU21 of the G-loop may stabilize the CDK2 complex by inducing a "close" conformation. This interaction likely explains the greater potency of compound **1** against CDK2 relative to compound **6m**.

We further evaluated the anticancer activity of compounds **2**, **6l**, and **6m** in other human cancer cell lines. As shown in Figure 3A, three compounds inhibited tumor cell proliferation at low micromolar concentrations in pancreatic cancer MIA Paca-2, colon cancer HCT116, and cervical cancer Hela cells. The antiproliferative activity of **6l** and **6m** was comparable to that of the parent compound **2** in both MIA Paca-2 and HCT116 cells. However, the IC_{50} values of two new analogs are two- to five-fold lower than that of compound **2** in Hela cells. We also investigated the effect of these compounds on the survival of two nontumorous cell lines. The IC_{50} values of all compounds are higher in embryonic mouse fibroblasts NIH3T3 and human umbilical vein endothelial cells (HUVEC) than the values in cancer cell lines. This suggests that these nontumorous cells are less sensitive to compound treatments than cancer cells (Figure 3A). Together, novel and selective CDK4/9 inhibitors were obtained through two rounds of SAR optimization, and several inhibitors demonstrated comparable anticancer activity compared to that of the parent compound and improved metabolic stability *in vitro*.

The bromodomain and extra terminal (BET) family bromodomain (BRD) proteins are important regulatory factors of oncogene c-Myc.[32] The first generation BET inhibitors represented by JQ1 have established the solid proof for BET bromodomain inhibition in cancer treatment.[33,34] However, short systemic exposure limits their clinical use, and relatively high doses increased unnecessary toxicities.[35] Some studies have indicated that the off-target effect of BET inhibitor might result from the activation of P-TEFb-dependent transcription.[36] Therefore, a number of studies have reported the potential therapeutic value of BET inhibitors in combination treatment in cancers, including their use with CDK9 inhibitors.[37−41] Here, we investigated whether our CDK4/9 inhibitor has an additive effect on the antiproliferative potency of JQ1. As shown in Figure 3B, coadministration of compound **6m** (1 μM) with JQ1 in varied concentrations ranging from 1 to 4 μM in HepG2 cells for 48 h significantly reduced cell viability compared to either single-agent treatment. This suggests that combining compound **6m** with JQ1 could synergistically enhance the antitumor efficacy.

We also investigated possible synergistic effects between **6m** and other anticancer agents including the Bcl-2 inhibitor

https://doi.org/10.1021/acsmedchemlett.6c00004
ACS Med. Chem. Lett. XXXX, XXX, XXX−XXX

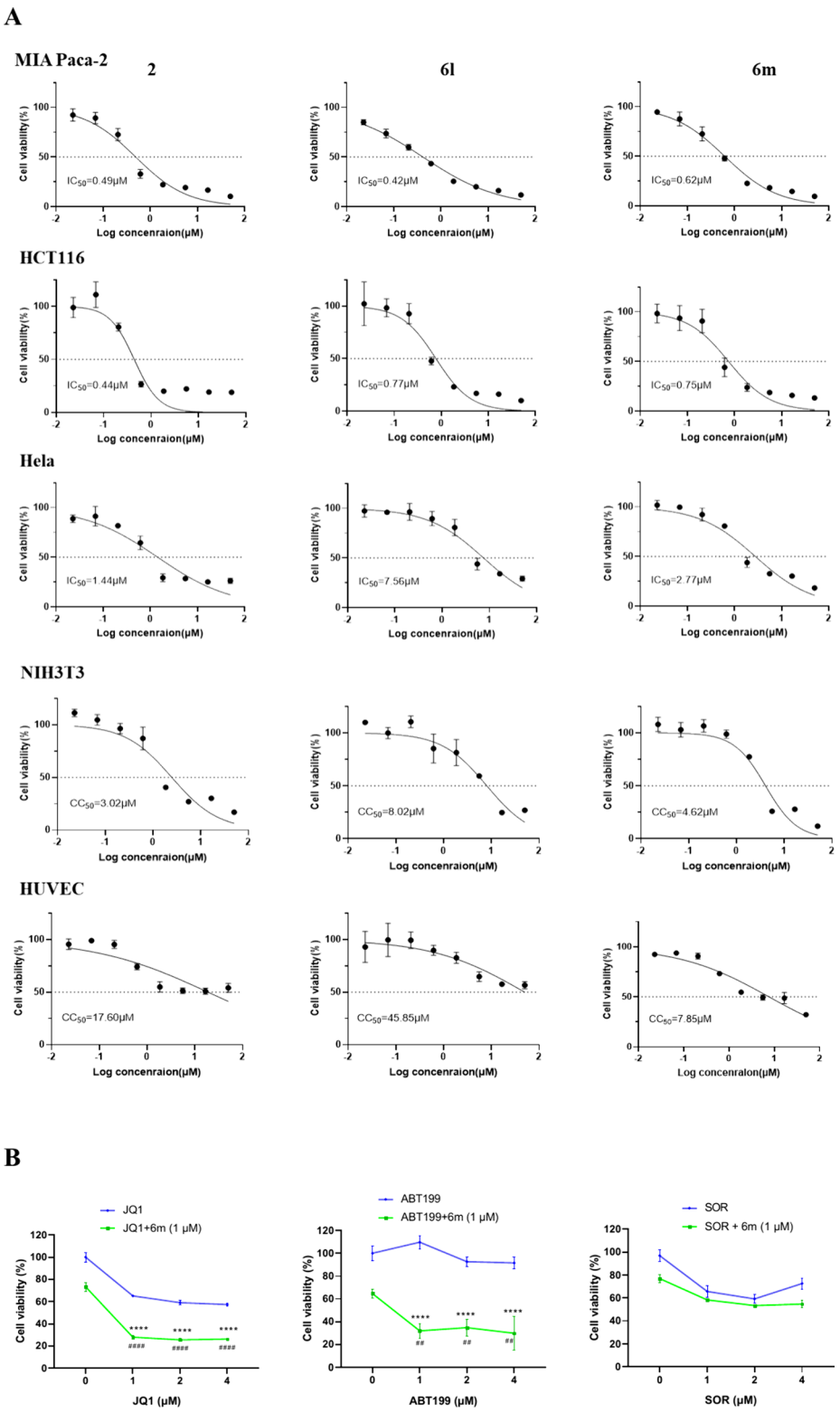

Figure 3. Novel pyrrolo[2,3-*d*]pyrimidine derivatives inhibited the proliferation of various cancer cell lines after both single and combination administrations. (A) Dose−response curves of the representative pyrrolo[2,3-*d*]pyrimidine derivatives in various cell lines. Cell viability was determined after 72h drug exposure by the MTT method (n = 3). (B) Drug combination effect of **6m** with JQ1, ABT199, or SOR on the proliferation of HepG2 cells. Cell viability was determined after 48 h drug exposure by MTT method. Data was presented as mean ± SD and the curves fitted by GraphPad software. **** means $p < 0.0001$ vs single drug dot in blue curves; $^{\#\#}$ and $^{\#\#\#\#}$ means $p < 0.01$ and $p < 0.0001$ vs **6m** single treatment, respectively (n = 3).

ABT199 and TKI drug sorafenib (SOR). The results showed that compound **6m** significantly increased the sensitivity of HepG2 cells to ABT199, and the combination of **6m** with ABT199 exhibited a stronger synergistic effect than that of its combination with JQ1 (Figure 3B, middle). This is consistent with previously described synergistic strategies combining Bcl-

https://doi.org/10.1021/acsmedchemlett.6c00004
ACS Med. Chem. Lett. XXXX, XXX, XXX−XXX

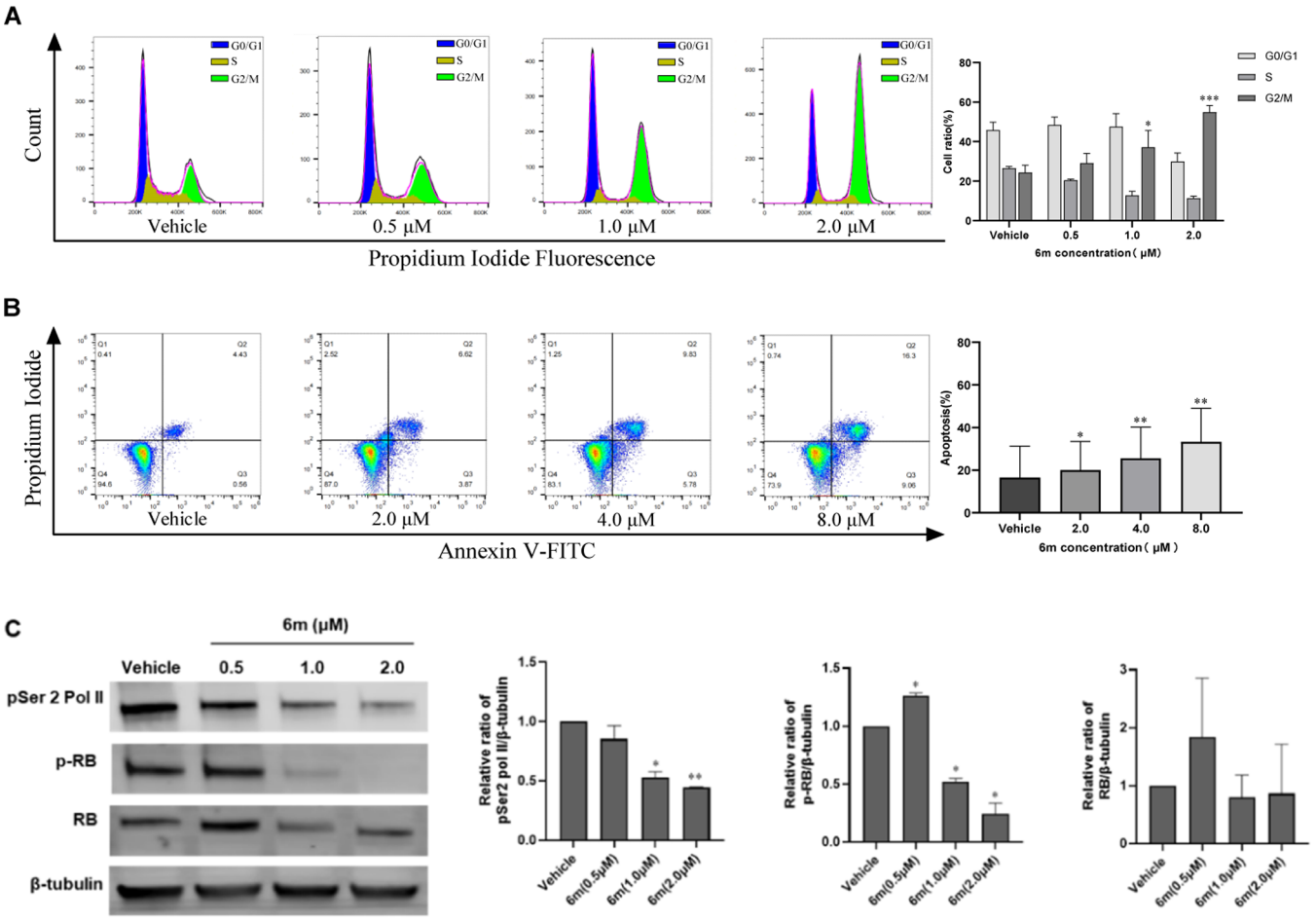

Figure 4. CDK4/9 inhibitor **6m** induced cell cycle arrest and apoptosis. (A) Cell cycle distribution was detected by propidium iodide (PI) staining and analyzed by flow cytometry. (B) Apoptosis was determined by annexinV-FITC/PI staining. (C) The effect of **6m** on the phosphorylation level of cellular RNA Pol II and the Rb protein. HepG2 cells were incubated with vehicle or **6m** at indicated concentrations for 24 h. Cellular protein level was determined by Western blot imaging, and representative protein bands from two independent experiments were quantified and normalized by internal reference protein β-tubulin. Quantification of data was shown in column graph. * $p < 0.05$, ** $p < 0.01$, *** $p < 0.001$, vs vehicle group ($n = 2$).

2 inhibitors with agents that down-regulate Mcl-1, as elevated Mcl-1 protein levels have been observed in ABT199-resistant cancer cell lines and primary patient samples.[42−44] In contrast, under the same experimental conditions, the additive effect of combining **6m** with TKI sorafenib in HepG2 cells was negligible. These results underscore the therapeutic potential of the selective CDK4/9 inhibitors in combination therapy.

Based on the above results, compound **6m** was further examined for its effect on the cell cycle. As shown in Figure 4, **6m** induced a dose-dependent increase in the G2-M content at concentrations ranging from 0.5 to 2.0 μM (Figure 4A). Moreover, a dose-dependent cell death occurred after 24 h of treatment with **6m** at higher concentrations (Figure 4B). This suggests that **6m** inhibits cancer cell proliferation by inducing both cell cycle arrest and apoptosis.

We also investigated the effect of compound **6m** on the cellular phosphorylation levels of retinoblastoma (Rb) protein and RNA polymerase II (RNA Pol II), whose upstream kinases are CDK4 and CDK9, respectively. The C-terminal domain (CTD) of RNA Pol II is generally phosphorylated at Ser2 (pSer2) by CDK9.[45] Dual inhibition of CDK4 and CDK9 by compound **6m** reduced the levels of phosphorylated Rb (p-Rb) and pSer2 Pol II in a dose-dependent manner while the total Rb protein expression remained relatively stable (Figure 4C). The dose-dependent decrease in these phosphorylated proteins is consistent with the antiproliferative potency of compound **6m** in HepG2 cells, indicating that its anticancer effects are attributed to the inhibition of CDK4 and CDK9 kinase activity.

To investigate the oral pharmacokinetic (PK) properties of newly synthesized pyrrolo[2,3-*d*]pyrimidine derivatives, plasma concentrations of compound **6m** were determined in mice at different time points following a single intravenous (IV, 5 mg/kg) or oral (PO, 25 mg/kg) dose. As shown in Figure 5, **6m** was rapidly absorbed into the blood circulation after oral administration, reaching Cmax within 1 h. Moreover, **6m** remained detectable in mouse plasma even 24 h after drug administration regardless of the administration route. The mean retention time (MRT) of **6m** was comparable between PO and IV administration. The half-life ($t_{1/2}$) of **6m** was shorter ($t_{1/2}$ = 4.6 h) after oral dosing than after intravenous dosing ($t_{1/2}$ = 6.4 h), suggesting the influence of enterohepatic circulation on its metabolism. The calculated peak plasma concentration of **6m** after oral dosing is 1205 ng/mL, which is several-fold higher than its IC_{50} values in HepG2, MIA Paca-2, and HCT116 cells. The *in vivo* residence duration for plasma concentrations beyond the *in vitro* IC_{50} was approximately 4 h in mice. Eventually, the area under the curve (AUC) after oral

https://doi.org/10.1021/acsmedchemlett.6c00004
ACS Med. Chem. Lett. XXXX, XXX, XXX−XXX

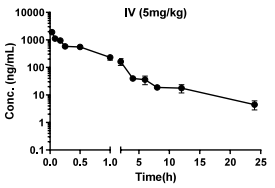

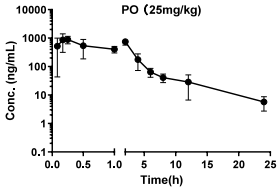

Parameter	Units	IV	PO
Dose	mg/kg	5	25
$AUC_{(0-t)}$	h*ng/mL	1376 ± 75.2	2758 ± 381
$MRT_{(0-t)}$	h	3.16 ± 0.29	3.38 ± 0.57
$t_{1/2z}$	h	6.49 ± 1.16	4.60 ± 2.27
t_{max}	h	0.03 ± 0	0.65 ± 0.90
C_{max}	ng/mL	1903 ± 229	1205 ± 143
Vz	mL/kg	32812 ± 4354	57823 ± 24669
CL	mL/h/kg	3535 ± 240	9074 ± 1322
F	%		40.1

Figure 5. Plasma concentration−time curves and pharmacokinetic parameters of **6m** after single dose administration to male ICR mice (male, $n = 4$).

dosing was twice that after intravenous dosing, from which the oral availability (F) of **6m** was calculated to be 40%.

In conclusion, two rounds of structural optimization were performed to improve the target selectivity and metabolic stability of a 4-sulfonylphenylaminopyrrolo[2,3-*d*]pyrimidine-based pan-CDK compound. SAR studies demonstrated that three new derivatives maintained *in vitro* antitumor activity while exhibiting improved metabolic stability and highly selective inhibition of CDK4 and CDK9 compared with the parent compound. These compounds possess broad-spectrum antitumor activity, with their antiproliferative effects resulting from cell cycle arrest and apoptosis induced by dual of CDK4/9 inhibition. Notably, one of the new derivatives demonstrated rapid oral absorption, prolonged residence time, and favorable oral bioavailability in *in vivo* PK studies. Moreover, combining this new derivative with BET or Bcl-2 inhibitors produced a synergistic anticancer effect. This study provides promising next-generation CDK inhibitor leads for the treatment of malignant solid tumors beyond breast cancer.

■ ASSOCIATED CONTENT

Supporting Information

The Supporting Information is available free of charge at https://pubs.acs.org/doi/10.1021/acsmedchemlett.6c00004.

Description of chemical synthesis procedures and characterization data, biological experimental protocols, and spectra graphs of synthetic compounds (PDF)

■ AUTHOR INFORMATION

Corresponding Authors

Zhuorong Li − *Institute of Medicinal Biotechnology, Chinese Academy of Medical Sciences & Peking Union Medical College, Beijing 100050, China;* orcid.org/0000-0001-5748-7444; Email: lizhurong@imb.pumc.edu.cn

Jinping Hu − *Institute of Materia Medica, Chinese Academy of Medical Sciences & Peking Union Medical College, Beijing 100050, China;* orcid.org/0000-0003-2382-2034; Email: hujp@imm.ac.cn

Yanping Li − *Institute of Medicinal Biotechnology, Chinese Academy of Medical Sciences & Peking Union Medical College, Beijing 100050, China;* orcid.org/0000-0002-5771-0252; Email: liyanping@imb.pumc.edu.cn

Authors

Siqi Li − *Institute of Medicinal Biotechnology, Chinese Academy of Medical Sciences & Peking Union Medical College, Beijing 100050, China*

Xiaotang Yang − *Institute of Medicinal Biotechnology, Chinese Academy of Medical Sciences & Peking Union Medical College, Beijing 100050, China*

Weiyi Yin − *Institute of Medicinal Biotechnology, Chinese Academy of Medical Sciences & Peking Union Medical College, Beijing 100050, China*

Wencui Zhang − *Institute of Medicinal Biotechnology, Chinese Academy of Medical Sciences & Peking Union Medical College, Beijing 100050, China*

Complete contact information is available at: https://pubs.acs.org/10.1021/acsmedchemlett.6c00004

Author Contributions

[§]Siqi Li and Xiaotang Yang contributed equally to this work.

Notes

The authors declare no competing financial interest.
No unexpected or unusually high safety hazards were encountered.

■ ACKNOWLEDGMENTS

This work is financially supported by CAMS Innovation Fund for Medical Sciences (2021-I2M-1-048).

■ ABBREVIATIONS

CDK, cyclin-dependent kinase; HCC, hepatocellular carcinoma; TKI, tyrosine kinase inhibitor; P-TEFb, positive transcription elongation factor b; SAR, structure−activity relationship; LMS, liver microsome stability; AURKA, aurora kinase A; BET, bromodomain and extra terminal; BRD, bromodomain; p-Rb, phosphorylated retinoblastoma; PI, propidium iodide

■ REFERENCES

(1) Sung, H.; Ferlay, J.; Siegel, R. L.; Laversanne, M.; Soerjomataram, I.; Jemal, A.; Bray, F. Global Cancer Statistics 2020: GLOBOCAN Estimates of Incidence and Mortality Worldwide for 36 Cancers in 185 Countries. *CA: A Cancer Journal for Clinicians* **2021**, *71* (3), 209−249.

(2) Zhou, J.; Sun, H.; Wang, Z.; Cong, W.; Zeng, M.; Zhou, W.; Liu, L.; Wen, T.; Kuang, M.; Zhang, B.; Tao, K.; Han, G.; Yan, Z.; Wang, M.; Liu, R.; Guo, J.; Zeng, Z.; Liang, P.; Ren, Z.; Hou, J.; Zhang, Y.; Liu, X.; Pan, H.; Bi, F.; Liang, C.; Chen, M.; Yan, F.; Xu, H.; Xie, X.; Ju, S.; Ji, Y.; Yun, J.; Li, Z.; Bai, X.; Cai, D.; Chen, W.; Chen, Y.; Chen, Y.; Cheng, W.; Cheng, S.; Dai, Z.; Dai, C.; Gao, Q.; Guo, R.; Guo, W.; Guo, Y.; Hua, B.; Huang, X.; Jiang, H.; Jia, W.; Li, Q.; Li, T.; Li, X.; Li, X.; Li, Y.; Li, Y.; Liang, J.; Liang, X.; Ling, C.; Liu, H.; Liu, T.; Lu, S.; Lv, G.; Mao, Y.; Meng, Z.; Peng, T.; Ren, W.; Shi, G.; Shi, H.; Shi, M.; Song, T.; Tan, G.; Wang, J.; Wang, K.; Wang, L.; Wang, W.; Wang, X.; Wang, Z.; Xiang, B.; Xia, J.; Xing, B.; Xu, J.; Xu, J.; Yang, J.; Yang, X.; Yang, Y.; Yang, Y.; Yao, X.; Yin, Z.; Yuan, Z.; Zeng, Y.; Zeng, Y.; Zhang, B.; Zhang, L.; Zhang, S.; Zhang, T.; Zhang, Z.; Zhao, M.; Zhao, Y.; Zheng, H.; Zhou, L.; Zhu, J.; Zhu, K.; Shi, Y.; Liu, R.; Zhang, L.; Xiao, Y.; Yang, C.; Wu, Z.; Ding, Z.; Zhu, X.; Tang, Z.;

Huang, X.; Han, H.; Wu, H.; Chen, M.; Wang, W.; Li, Q.; Cai, J.; Shen, F.; Cai, X.; Qin, S.; Teng, G.; Fan, J. China Liver Cancer Guidelines for the Diagnosis and Treatment of Hepatocellular Carcinoma (2024 Edition). *Liver Cancer* **2025**, 1.

(3) Abou-Alfa, G. K.; Meyer, T.; Cheng, A.-L.; El-Khoueiry, A. B.; Rimassa, L.; Ryoo, B.-Y.; Cicin, I.; Merle, P.; Chen, Y.; Park, J.-W.; Blanc, J.-F.; Bolondi, L.; Klümpen, H.-J.; Chan, S. L.; Zagonel, V.; Pressiani, T.; Ryu, M.-H.; Venook, A. P.; Hessel, C.; Borgman-Hagey, A. E.; Schwab, G.; Kelley, R. K. Cabozantinib in Patients with Advanced and Progressing Hepatocellular Carcinoma. *New England Journal of Medicine* **2018**, *379* (1), 54−63.

(4) Bruix, J.; Qin, S.; Merle, P.; Granito, A.; Huang, Y.-H.; Bodoky, G.; Pracht, M.; Yokosuka, O.; Rosmorduc, O.; Breder, V.; Gerolami, R.; Masi, G.; Ross, P. J.; Song, T.; Bronowicki, J.-P.; Ollivier-Hourmand, I.; Kudo, M.; Cheng, A.-L.; Llovet, J. M.; Finn, R. S.; LeBerre, M.-A.; Baumhauer, A.; Meinhardt, G.; Han, G. Regorafenib for patients with hepatocellular carcinoma who progressed on sorafenib treatment (RESORCE): a randomised, double-blind, placebo-controlled, phase 3 trial. *Lancet* **2017**, *389* (10064), 56−66.

(5) Kudo, M.; Finn, R. S.; Qin, S.; Han, K.-H.; Ikeda, K.; Piscaglia, F.; Baron, A.; Park, J.-W.; Han, G.; Jassem, J.; Blanc, J. F.; Vogel, A.; Komov, D.; Evans, T. R. J.; Lopez, C.; Dutcus, C.; Guo, M.; Saito, K.; Kraljevic, S.; Tamai, T.; Ren, M.; Cheng, A.-L. Lenvatinib versus sorafenib in first-line treatment of patients with unresectable hepatocellular carcinoma: a randomised phase 3 non-inferiority trial. *Lancet* **2018**, *391* (10126), 1163−1173.

(6) Zhu, A. X.; Park, J. O.; Ryoo, B.-Y.; Yen, C.-J.; Poon, R.; Pastorelli, D.; Blanc, J.-F.; Chung, H. C.; Baron, A. D.; Pfiffer, T. E. F.; Okusaka, T.; Kubackova, K.; Trojan, J.; Sastre, J.; Chau, I.; Chang, S.-C.; Abada, P. B.; Yang, L.; Schwartz, J. D.; Kudo, M. Ramucirumab versus placebo as second-line treatment in patients with advanced hepatocellular carcinoma following first-line therapy with sorafenib (REACH): a randomised, double-blind, multicentre, phase 3 trial. *Lancet Oncology* **2015**, *16* (7), 859−870.

(7) Vogel, A.; Meyer, T.; Sapisochin, G.; Salem, R.; Saborowski, A. Hepatocellular carcinoma. *Lancet* **2022**, *400* (10360), 1345−1362.

(8) Feng, M. Y.; Chan, L. L.; Chan, S. L. Drug Treatment for Advanced Hepatocellular Carcinoma: First-Line and Beyond. *Curr. Oncol* **2022**, *29* (8), 5489−5507.

(9) Vogel, A.; Saborowski, A. Current strategies for the treatment of intermediate and advanced hepatocellular carcinoma. *Cancer Treatment Reviews* **2020**, *82*, 101946.

(10) Colagrande, S. Advanced hepatocellular carcinoma and sorafenib: Diagnosis, indications, clinical and radiological follow-up. *World Journal of Hepatology* **2015**, *7* (8), 1041.

(11) Siegel, R. L.; Miller, K. D.; Fuchs, H. E.; Jemal, A. Cancer Statistics, 2021. *CA Cancer J. Clin* **2021**, *71* (1), 7−33.

(12) Malumbres, M. Cyclin-dependent kinases. *Genome Biol.* **2014**, *15* (6), 122.

(13) Malumbres, M.; Barbacid, M. To cycle or not to cycle: a critical decision in cancer. *Nat. Rev. Cancer* **2001**, *1* (3), 222−31.

(14) Morgan, D. O. Principles of CDK regulation. *Nature* **1995**, *374* (6518), 131−4.

(15) Mounika, P.; Gurupadayya, B.; Kumar, H. Y.; Namitha, B. An Overview of CDK Enzyme Inhibitors in Cancer Therapy. *Current Cancer Drug Targets* **2023**, *23* (8), 603−619.

(16) Shi, Z.; Tian, L.; Qiang, T.; Li, J.; Xing, Y.; Ren, X.; Liu, C.; Liang, C. From Structure Modification to Drug Launch: A Systematic Review of the Ongoing Development of Cyclin-Dependent Kinase Inhibitors for Multiple Cancer Therapy. *J. Med. Chem.* **2022**, *65* (9), 6390−6418.

(17) O'Leary, B.; Finn, R. S.; Turner, N. C. Treating cancer with selective CDK4/6 inhibitors. *Nat. Rev. Clin Oncol* **2016**, *13* (7), 417−30.

(18) Goodwin, C. M.; Waters, A. M.; Klomp, J. E.; Javaid, S.; Bryant, K. L.; Stalnecker, C. A.; Drizyte-Miller, K.; Papke, B.; Yang, R.; Amparo, A. M.; Ozkan-Dagliyan, I.; Baldelli, E.; Calvert, V.; Pierobon, M.; Sorrentino, J. A.; Beelen, A. P.; Bublitz, N.; Luthen, M.; Wood, K. C.; Petricoin, E. F.; Sers, C.; McRee, A. J.; Cox, A. D.; Der, C. J. Combination Therapies with CDK4/6 Inhibitors to Treat KRAS-Mutant Pancreatic Cancer. *Cancer Res.* **2023**, *83* (1), 141−157.

(19) Ngamphaiboon, N.; Pattaranutaporn, P.; Lukerak, S.; Siripoon, T.; Jinawath, A.; Arsa, L.; Shantavasinkul, P. C.; Taonam, N.; Trachu, N.; Jinawath, N.; Kositwattanarerk, A.; Sananmuang, T.; Jiarpinitnun, C. A Phase I Study of the CDK4/6 Inhibitor Palbociclib in Combination with Cetuximab and Radiotherapy for Locally Advanced Head and Neck Squamous Cell Carcinoma. *Clin. Cancer Res.* **2024**, *30* (2), 294−303.

(20) Martin, P.; Ruan, J.; Furman, R.; Rutherford, S.; Allan, J.; Chen, Z.; Huang, X.; DiLiberto, M.; Chen-Kiang, S.; Leonard, J. P. A phase I trial of palbociclib plus bortezomib in previously treated mantle cell lymphoma. *Leuk Lymphoma* **2019**, *60* (12), 2917−2921.

(21) Grana, X.; De Luca, A.; Sang, N.; Fu, Y.; Claudio, P. P.; Rosenblatt, J.; Morgan, D. O.; Giordano, A. PITALRE, a nuclear CDC2-related protein kinase that phosphorylates the retinoblastoma protein in vitro. *Proc. Natl. Acad. Sci. U. S. A.* **1994**, *91* (9), 3834−8.

(22) Fujinaga, K.; Huang, F.; Peterlin, B. M. P-TEFb: The master regulator of transcription elongation. *Mol. Cell* **2023**, *83* (3), 393−403.

(23) Wang, S.; Fischer, P. M. Cyclin-dependent kinase 9: a key transcriptional regulator and potential drug target in oncology, virology and cardiology. *Trends Pharmacol. Sci.* **2008**, *29* (6), 302−13.

(24) Diamond, J. R.; Boni, V.; Lim, E.; Nowakowski, G.; Cordoba, R.; Morillo, D.; Valencia, R.; Genvresse, I.; Merz, C.; Boix, O.; Frigault, M. M.; Greer, J. M.; Hamdy, A. M.; Huang, X.; Izumi, R.; Wong, H.; Moreno, V. First-in-Human Dose-Escalation Study of Cyclin-Dependent Kinase 9 Inhibitor VIP152 in Patients with Advanced Malignancies Shows Early Signs of Clinical Efficacy. *Clin. Cancer Res.* **2022**, *28* (7), 1285−1293.

(25) Wu, T.; Wu, X.; Xu, Y.; Chen, R.; Wang, J.; Li, Z.; Bian, J. A patent review of selective CDK9 inhibitors in treating cancer. *Expert Opin Ther Pat* **2023**, *33* (4), 309−322.

(26) Hanna, G. J.; Cote, G. M.; Chugh, R.; Thomas, J. S.; Malhotra, J.; Cutler, R. E.; Hood, T.; Carvajal, L. A.; Olek, E. A.; Villalona-Calero, M. A. Safety and Efficacy of a Selective Inhibitor of Cyclin-dependent Kinase 9 (KB-0742) in Patients with Recurrent or Metastatic Adenoid Cystic Carcinoma. *Cancer Res. Commun.* **2025**, *5* (5), 767−773.

(27) Yang, B.; Quan, Y.; Zhao, W.; Ji, Y.; Yang, X.; Li, J.; Li, Y.; Liu, X.; Wang, Y.; Li, Y. Design, synthesis and biological evaluation of 2-((4-sulfamoylphenyl)amino)-pyrrolo[2,3-d]pyrimidine derivatives as CDK inhibitors. *J. Enzyme Inhib Med. Chem.* **2023**, *38* (1), 2169282.

(28) Cai, D.; Latham, V. M., Jr.; Zhang, X.; Shapiro, G. I. Combined depletion of cell cycle and transcriptional cyclin-dependent kinase activities induces apoptosis in cancer cells. *Cancer Res.* **2006**, *66* (18), 9270−80.

(29) Palmer, C. L.; Boras, B.; Pascual, B.; Li, N.; Li, D.; Garza, S.; Huser, N.; Yuan, J. T.; Cianfrogna, J. A.; Sung, T.; McMillan, E.; Wei, N.; Carmody, J.; Kang, A. N.; Darensburg, S.; Dodd, T.; Oakley, J. V.; Solowiej, J.; Nguyen, L.; Orr, S. T. M.; Chen, P.; Johnson, E.; Yu, X.; Diehl, W. C.; Gallego, G. M.; Jalaie, M.; Ferre, R. A.; Cho-Schultz, S.; Shen, H.; Deal, J. G.; Zhang, Q.; Baffi, T. R.; Xu, M.; Roh, W.; Lapira-Miller, J.; Goudeau, J.; Yu, Y.; Gupta, R.; Kim, K.; Dann, S. G.; Kan, Z.; Kath, J. C.; Nair, S. K.; Miller, N.; Murray, B. W.; Nager, A. R.; Quinlan, C.; Petroski, M. D.; Zhang, C.; Sacaan, A.; VanArsdale, T.; Anders, L. CDK4 selective inhibition improves preclinical anti-tumor efficacy and safety. *Cancer Cell* **2025**, *43* (3), 464−481 e14.

(30) Maddeboina, K.; Pal, D.; Yada, B.; McHale, C. C.; Singh, S. K.; Chhonker, Y. S.; Dryden, H. L.; Delara, R.; Mujumdar, V.; Zhang, Q.; Murry, D. J.; Durden, D. L. Discovery of a "First-in-Class" Selective Multikinase (CDK4/6/9-AURKA/B) Inhibitor, LCI133, for Neuroblastoma. *J. Med. Chem.* **2025**, *68* (22), 24024−24046.

(31) Jiang, C.; Ye, Y.; Kang, W.; Yang, J.; He, Z.; Cao, Q.; Lian, C.; Xing, Y.; Yang, Q.; Zhao, J.; Pan, S.; Feng, M.; Song, C.; Liu, Z.; Wang, R.; Yin, F.; Wu, Y. D.; Chen, J.; Huang, Y. Elucidating Binding Selectivity in Cyclin-Dependent Kinases 4, 6, and 9: Development of Highly Potent and Selective CDK4/9 Inhibitors. *J. Med. Chem.* **2025**, *68* (2), 1499−1510.

https://doi.org/10.1021/acsmedchemlett.6c00004
ACS Med. Chem. Lett. XXXX, XXX, XXX−XXX

(32) Wu, X.; Liu, D.; Gao, X.; Xie, F.; Tao, D.; Xiao, X.; Wang, L.; Jiang, G.; Zeng, F. Inhibition of BRD4 Suppresses Cell Proliferation and Induces Apoptosis in Renal Cell Carcinoma. *Cell Physiol Biochem* **2017**, *41* (5), 1947−1956.
(33) Delmore, J. E.; Issa, G. C.; Lemieux, M. E.; Rahl, P. B.; Shi, J.; Jacobs, H. M.; Kastritis, E.; Gilpatrick, T.; Paranal, R. M.; Qi, J.; Chesi, M.; Schinzel, A. C.; McKeown, M. R.; Heffernan, T. P.; Vakoc, C. R.; Bergsagel, P. L.; Ghobrial, I. M.; Richardson, P. G.; Young, R. A.; Hahn, W. C.; Anderson, K. C.; Kung, A. L.; Bradner, J. E.; Mitsiades, C. S. BET bromodomain inhibition as a therapeutic strategy to target c-Myc. *Cell* **2011**, *146* (6), 904−17.
(34) Filippakopoulos, P.; Qi, J.; Picaud, S.; Shen, Y.; Smith, W. B.; Fedorov, O.; Morse, E. M.; Keates, T.; Hickman, T. T.; Felletar, I.; Philpott, M.; Munro, S.; McKeown, M. R.; Wang, Y.; Christie, A. L.; West, N.; Cameron, M. J.; Schwartz, B.; Heightman, T. D.; La Thangue, N.; French, C. A.; Wiest, O.; Kung, A. L.; Knapp, S.; Bradner, J. E. Selective inhibition of BET bromodomains. *Nature* **2010**, *468* (7327), 1067−73.
(35) Lewin, J.; Soria, J. C.; Stathis, A.; Delord, J. P.; Peters, S.; Awada, A.; Aftimos, P. G.; Bekradda, M.; Rezai, K.; Zeng, Z.; Hussain, A.; Perez, S.; Siu, L. L.; Massard, C. Phase Ib Trial With Birabresib, a Small-Molecule Inhibitor of Bromodomain and Extraterminal Proteins, in Patients With Selected Advanced Solid Tumors. *J. Clin Oncol* **2018**, *36* (30), 3007−3014.
(36) Mota de Sa, P.; Richard, A. J.; Stephens, J. M. Bromodomain and Extraterminal Inhibition by JQ1 Produces Divergent Transcriptional Regulation of Suppressors of Cytokine Signaling Genes in Adipocytes. *Endocrinology* **2020**, *161* (2). DOI: 10.1210/endocr/bqz034.
(37) Cancer, M.; Drews, L. F.; Bengtsson, J.; Bolin, S.; Rosen, G.; Westermark, B.; Nelander, S.; Forsberg-Nilsson, K.; Uhrbom, L.; Weishaupt, H.; Swartling, F. J. BET and Aurora Kinase A inhibitors synergize against MYCN-positive human glioblastoma cells. *Cell Death Dis* **2019**, *10* (12), 881.
(38) Marr, A. R.; Halpin, M.; Corbin, D. L.; Asemelash, Y.; Sher, S.; Gordon, B. K.; Whipp, E. C.; Mitchell, S.; Harrington, B. K.; Orwick, S.; Benrashid, S.; Goettl, V. M.; Yildiz, V.; Mitchell, A. D.; Cahn, O.; Mims, A. S.; Larkin, K. T. M.; Long, M.; Blachly, J.; Woyach, J. A.; Lapalombella, R.; Grieselhuber, N. R. The multi-CDK inhibitor dinaciclib reverses bromo- and extra-terminal domain (BET) inhibitor resistance in acute myeloid leukemia via inhibition of Wnt/beta-catenin signaling. *Exp Hematol Oncol* **2024**, *13* (1), 27.
(39) Carra, G.; Nicoli, P.; Lingua, M. F.; Maffeo, B.; Cartella, A.; Circosta, P.; Brancaccio, M.; Parvis, G.; Gaidano, V.; Guerrasio, A.; Saglio, G.; Taulli, R.; Morotti, A. Inhibition of bromodomain and extra-terminal proteins increases sensitivity to venetoclax in chronic lymphocytic leukaemia. *J. Cell Mol. Med.* **2020**, *24* (2), 1650−1657.
(40) Karakashev, S.; Zhu, H.; Yokoyama, Y.; Zhao, B.; Fatkhutdinov, N.; Kossenkov, A. V.; Wilson, A. J.; Simpkins, F.; Speicher, D.; Khabele, D.; Bitler, B. G.; Zhang, R. BET Bromodomain Inhibition Synergizes with PARP Inhibitor in Epithelial Ovarian Cancer. *Cell Rep* **2017**, *21* (12), 3398−3405.
(41) Kuang, Z.; Guo, K.; Cao, Y.; Jiang, M.; Wang, C.; Wu, Q.; Hu, G.; Ao, M.; Huang, M.; Qin, J.; Zhao, T.; Lu, S.; Sun, C.; Li, M.; Wu, T.; Liu, W.; Fang, M. The novel CDK9 inhibitor, XPW1, alone and in combination with BRD4 inhibitor JQ1, for the treatment of clear cell renal cell carcinoma. *Br. J. Cancer* **2023**, *129* (12), 1915−1929.
(42) Tahir, S. K.; Smith, M. L.; Hessler, P.; Rapp, L. R.; Idler, K. B.; Park, C. H.; Leverson, J. D.; Lam, L. T. Potential mechanisms of resistance to venetoclax and strategies to circumvent it. *BMC Cancer* **2017**, *17* (1), 399.
(43) Niu, X.; Zhao, J.; Ma, J.; Xie, C.; Edwards, H.; Wang, G.; Caldwell, J. T.; Xiang, S.; Zhang, X.; Chu, R.; Wang, Z. J.; Lin, H.; Taub, J. W.; Ge, Y. Binding of Released Bim to Mcl-1 is a Mechanism of Intrinsic Resistance to ABT-199 which can be Overcome by Combination with Daunorubicin or Cytarabine in AML Cells. *Clin. Cancer Res.* **2016**, *22* (17), 4440−51.
(44) Luedtke, D. A.; Su, Y.; Ma, J.; Li, X.; Buck, S. A.; Edwards, H.; Polin, L.; Kushner, J.; Dzinic, S. H.; White, K.; Lin, H.; Taub, J. W.; Ge, Y. Inhibition of CDK9 by voruciclib synergistically enhances cell death induced by the Bcl-2 selective inhibitor venetoclax in preclinical models of acute myeloid leukemia. *Signal Transduct Target Ther* **2020**, *5* (1), 17.
(45) Garriga, J.; Grana, X. Cellular control of gene expression by T-type cyclin/CDK9 complexes. *Gene* **2004**, *337*, 15−23.

https://doi.org/10.1021/acsmedchemlett.6c00004
ACS Med. Chem. Lett. XXXX, XXX, XXX−XXX